Lunar Maria: Structure and Evolution

Abstract. *The lunar maria are considered to have evolved as homologous, transient, gravity-wave systems from large impact craters on a crustal layer 50 kilometers thick, fluidized from beneath by prompt, shock-induced melting inside an initially hot moon.*

The spacing of the five concentric mountain rings surrounding the lunar mare Orientale was shown to fit uniquely the dispersion curve for free gravity waves on a 50-km "liquid" layer overlying a rigid basement (*1*). I interpreted this to mean that, following violent disruption by the shock wave from the initiating impact explosion, the fragmented solid material in this layer possessed negligible rigidity or viscosity, tending to flow like a fluid for about an hour, and being ultimately arrested by elastic forces at a radius where the peak shock pressure had fallen below that necessary to produce fracturing (~ 1 kb). The evidence for partial ring structures around most of the maria, and their subsequent inundation in varying degree by what appear to be lavas upwelling from beneath, is an indication of their common origin as the result of impact explosions having sufficient energy to trigger spontaneous melting at depths of 100 to 200 km inside an initially hot moon.

I now present additional evidence that the 50-km layer was a universal feature of the lunar crustal structure at the time of mare formation by showing that the relatively abundant and widely distributed maria are homologous generic structures that are scalable in terms of impact energy. The extreme fluidity implied by the transient wave-like behavior of these ring systems may have been the result of prompt fluidization of the surface layer by injection of lava upward through shock-produced fissures in the substratum; the bulk of presently visible surface inundation occurred on a time scale which is the same as that for wave formation.

From the Orbiter photographs I have been able to identify tentatively over 40 multiring maria; these I elect to define as structures possessing two or more concentric mountain rings in which most of the central basins and portions of the spaces between the rings appear to have been smoothly flooded with lava. At least a dozen additional features deserve closer examination under this definition. The position coordinates and respective ring radii of 16 characteristic examples are listed in Table 1. The radii for the larger maria were determined independently by R. Eggleton (U.S. Geological Survey, Flagstaff) and by me, and correspond fairly closely with those reported by Hartmann and Kuiper (*2*), although we credit Imbrium with two more rings than are generally acknowledged, by presuming that the Carpathian-Apennine ring is a separate feature from the Alpine arc, and that both are concentric with the barely decipherable inner ring best identified by the Spitzbergen mountains. Although Serenitatis is defined by only a single ring, I have included it because it can tentatively be fitted into the general scheme on the basis of energetics.

That the tabulated ring data are consistent with the gravity-wave hypothesis is shown in Fig. 1, where the computed trajectories (smooth curves) for the first five crests from an impulsive disturbance propagating on a 50-km deep "liquid" layer are presented in a space-time coordinate system, according to the method of Van Dorn (*1*). The respective ring radii for each mare were then plotted along a separate strip of paper to the given ordinate scale, and the slip was moved horizontally along the time axis to obtain the best fit with the computed curves. The graphical solutions thus obtained are unique in that no other position of any slip gives a satisfactory fit. The intersections of these solutions (vertical dashed lines) with the time axis give the times of freezing (cessation of wave motion, assumed to be instantaneous) of the respective events, reckoned from the moment of impact. Agreement between the predicted curves and the observed data supports the conclusion that the 50-km layer proposed for Orientale was a general feature of the lunar crust during mare formation.

An estimate of the relative energetics of the above impacts can also be obtained from the Orientale model (*1*), in which the initial crater radius (50 km) was deduced from the spacing and relative heights of the five mountain rings, and the impact energy (1.4×10^{31} ergs) (*3*) was determined by normalizing an empirical radius-depth relation for explosion-craters to an impact-penetration model, based on the observed ejecta limits. The inferred crater radius depends sensitively upon

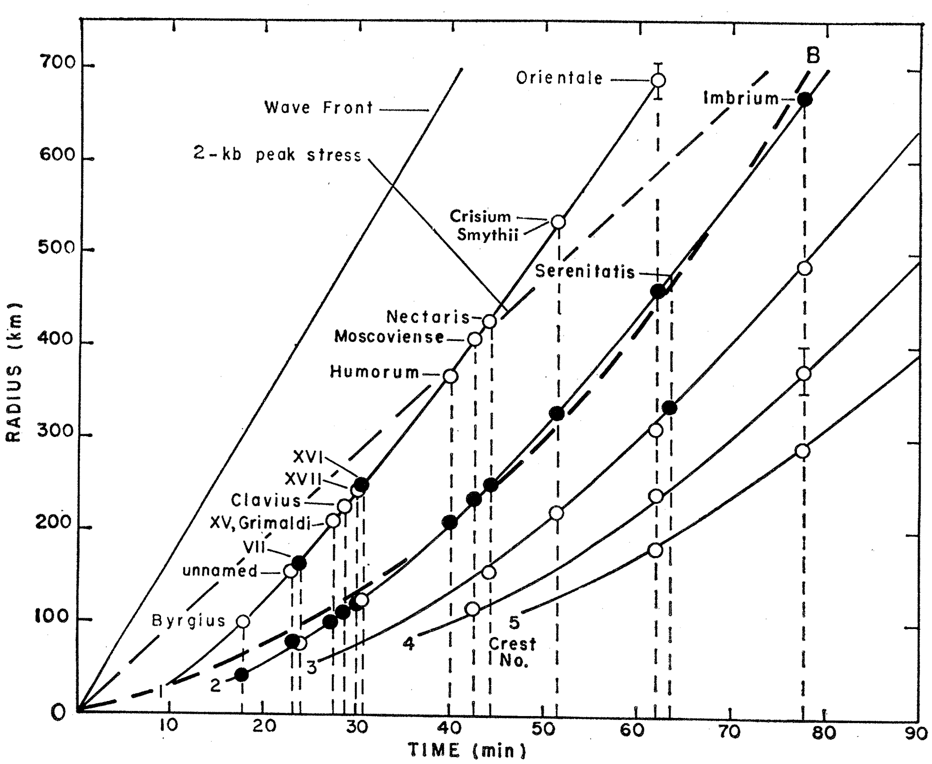

Fig. 1. Computed trajectories in space-time coordinates for wave front and first five wave crests propagating on 50-km lunar crustal layer. Vertical dashed lines, giving freezing times of maria, are best-fit solutions of observed ring spacing to predicted curves. Highest rings (filled circles) agree with predicted locus *O-B* of spectral maximum.

Table 1. Mare parameters.

Mare	Coordinates*		Crater radius (km)	Ring radii (km)*					Freezing time (min)	Impact energy (× 10^{31} ergs)
	Latitude	Longitude		1	2	3	4	5		
Imbrium	34°N	16°W	82		670	485	350	290	78	7.7
Serenitatis	27°N	19°E	56			335			63	4.5
Orientale	20°S	95°W	67	680	465	310	240	180	62	3.9
Smythii	01°N	81°E	56	530	335	225			51	2.2
Crisium	17°N	56°E	56	530	335	225			51	2.2
Nectaris	16°S	33°W	49	430	250	130			44	1.4
Moscoviense	24°N	146°E	48	410	235	215			43	1.2
Humorum	24°S	39°W	45	365	220				40	1.0
XVI	36°S	152°W	35	250	125				31	0.47
XVII	02°N	129°W	34	245	120				30	.43
Clavius	58°S	15°W	33	225	110				29	.39
XV	03°S	159°W	32	210	100				28	.31
Grimaldi	07°S	68°W	32	210	100				28	.31
VII	69°S	130°W	25	165	75				24	.22
Unnamed	56°S	44°W	24	158	80				23	.21
Byrgius	25°S	65°W	22	50	21				18	.10

* Indicates observed data.

the position of the peak of the amplitude spectrum, that is, upon which ring of the system is highest. In Fig. 1 the highest rings for the respective maria are indicated by closed circles, and in the majority of cases the second ring is highest. Ring 3 of Orientale (Rook Mountains) was earlier reported highest on the basis of scattered shadow measurements, but other photographs at low sun angles show abundant peak reflections from ring 2 (Cordilleras) at least as far into the terminator as those from ring 3. Therefore I have represented both points by closed circles in Fig. 1. This has the effect of moving the spectral maximum to a slightly lower frequency, and increasing the computed crater radius to 67 km and the impact energy to 3.9×10^{31} ergs.

If one now reasonably supposes that the freezing times for the maria represent times when their respective shock stresses have dropped to the same level within the region of wave motion, then the ratio of the freezing times for any two events should be proportional to the cube root of the ratio of their respective impact (explosion) energies. Secondly, the spectral amplitude maximum (region of highest waves) for explosion-generated surface waves in water of finite depth (*4*) is characterized by the invariant relation

$$r_0 W^{0.3} k^* = \text{constant}$$

where $r_0 W^{0.3}$ is the scaled radius of the explosion cavity, W is the explosion energy, and k^* is the wave number at the spectral maximum determined from observational data. This invariant relation has two conditions: that $k^*h \geqslant 2$ (h, liquid depth), and that the explosion depth beneath the free surface is similarly scaled. The first condition is satisfied for Orientale and all smaller events in a 50-km layer, and the results of studies of hypervelocity penetration (*1*) suggest that impact explosion depths are also suitably scaled.

Accordingly, I have computed k^* for the maria of Table 1, normalized to the energy deduced for Orientale, using the cited freezing times to determine their energies. The predicted locus of k^* is shown in Fig. 1 as the heavy dashed line *O-B*. From the general agreement between this line and the observed positions of the highest rings I conclude that the maria are indeed homologous structures, scalable in terms of impact energy. The respective freezing times, initial crater radii, and impact energies are also listed in Table 1.

From their common origin as impact events, Baldwin (*5*) and others have proposed that the maria are simply oversized craters, isostatically backfilled and subsequently flooded with lava over a long time span. It is commonly assumed that one or another of the mountain rings constitutes the vestigial remains of the flooded crater. Alternatively, the wave hypothesis suggests that the initial craters—deduced to be much smaller than the inner mountain rings (Table 1)—represent only a transient phase in the process of mare formation. In fact, the rings are thought to be formed by the potential flow resulting from complete collapse of the crater! Thus, craters, some of which appear to be substantially larger than the smaller mare rings, might be viewed as potential maria, prematurely arrested from evolution as wavelike ring structures by essential differences in the degree of fluidity induced in the surrounding material by a given impact. The maria are characterized by extremely fluidlike motions at an early stage and are invariably associated with abundant production of lava, whereas the postimpact motions of craters appear to be limited to slumping and partial backfilling. The distinction seems to be primarily, but not altogether, one of energetics. I propose that the maria evolved somewhat in accordance with the following scheme, and that exceptions can be accounted for by local or temporal departures from the assumed initial conditions.

Consider a hypothetical thermal model for the moon, at the time of mare formation, comprising a molten interior below 200 km overlaid successively upward by: (i) a 100-km eclogitic plastic layer wherein the temperatures are low enough and the pressures are high enough to inhibit phase transition to basalt; (ii) a 50-km elastic basalt layer warm enough to permit slow recrystallization by diffusion; and (iii) a 50-km unconsolidated, low-density, basaltic surface layer thoroughly turned into rubble by an extensive impact history. This model is sufficiently similar to models proposed by Anderson and Phinney (*6*) and Levin (*7*) to be plausible if minor adjustments of their initial premises are made. Similarly, the configuration envisaged could be substantially altered in scale without invalidating the substance of the following hypothesis.

An impact explosion within the surface layer of such a structure, sufficiently energetic to generate shock pressures substantially exceeding the ambient hydrostatic pressure within the elastic layer, would be expected to produce an extensive system of radial and peripheral fissures in the latter layer through the mechanism of spallation (*8*). Immediately after the passage of the shock front, the pressures within the plastic layer would drop to well below the ambient hydrostatic level because of the combined effects of shock rarefaction from the free surface and ejection of material from the explosion crater. Pressure relief would permit prompt, spontaneous melting through the unstable phase transition from eclogite to basalt to an extent limited only by the available latent superheat. The liquidus fraction, which is assumed to have somewhat lower density than the surface layer, abetted by inward collapse of the entire potential field interior to the (now distant) shock wave, would be injected upward at high velocity through the radial fissures to perfuse and fluidize the entire overlying surface layer. These motions, which would be most intense in the central region delimited by the explosion crater, would ensure the hydrodynamic collapse of the crater into an elevated mound, which would then subside to form the familiar ring system in the surrounding fluidized region. The radial extent of fluidlike motions, according to this model, would be limited to that radius where the initial peak shock pressure had degraded to the order of the ambient hydrostatic pressure at the top of the elastic layer ($\sim$ 2 kb). This limit, which scales like the cube-root of explosion energy, is shown (Fig. 1) as a reasonable bound to the observed ring systems.

After generation of the rings and the restoration of hydrostatic equilibrium, I suggest that relatively slow isostatic collapse of the rings was prevented, or mitigated, by more rapid resolidification of the perfused rubble-fluid matrix within the surface layer, where the rapid heat transfer to the solid phase would occur during the period of fluidization (20 to 80 minutes). However, I expect that the central region, being relatively enriched with injected material, would remain plastic for a much longer time, and hence would be in quasi-isostatic equilibrium with the plastic region below. Eventual cooling by conduction through the surface would result in a solid layer of somewhat higher density whose strength-weight ratio would increase roughly as the square of its thickness, possibly resulting in a self-supporting structure. Subsequent smaller impacts into such a structure, before complete subsurface freezing had occurred, would be expected to produce the partially flooded craters characterized by Archimedes and Plato within the central basin of Mare Imbrium.

While the foregoing model invokes hydrodynamic and thermodynamic processes on a scale totally beyond human experience, none of them is mysterious, and most of them are amenable to experiment or calculation. The extreme fluidity necessary to sustain surface waves and the enormous heat transfer rates required to freeze them are well-known properties of fluidized liquid-solid systems (*9*). Numerical methods for the analysis of explosive cratering have already been applied to hyper-velocity impacts into homogeneous material (*10*). Their extension to the proposed multilayer model would be of great interest. If the epoch of mare formation occurred during the moon's cooling phase, at least the predicted 50-km discontinuity should still be detectable by seismic refraction in regions outside the maria; if mare formation occurred during the heating phase, I would expect to find the discontinuity at some shallower depth.

W. G. VAN DORN
Scripps Institution of Oceanography, University of California, San Diego, La Jolla 92037

References and Notes

1. W. G. Van Dorn, *Nature* **220**, 1102 (1968).
2. W. K. Hartmann and G. P. Kuiper, *Commun. Lunar Planet. Lab. Univ. Ariz.* **1**, 12 (1962).
3. Erroneously reported in (*1*) as 1.4×10^{30} ergs.
4. W. G. Van Dorn, B. Le Mehaute, L. Hwang, *Handbook of Explosion-Generated Waves* (Spec. Rep. TC-130, Tetra Tech, Inc., Pasadena, 1968), p. 26.
5. R. B. Baldwin, *Science* **162**, 1407 (1968).
6. D. L. Anderson and R. A. Phinney, in *Mantles of the Earth and Planets*, S. K. Rincorn, Ed. (Wiley, New York, 1967), p. 124.
7. J. Levin, in *The Nature of the Lunar Surface*, W. Hess, D. Menzel, J. O'Keefe, Eds. (Johns Hopkins Press, Baltimore, 1965), pp. III–15.
8. M. D. Nordyke, *J. Geophys. Res.* **66**, 3439 (1961).
9. J. D. Murray, *J. Fluid Mech.* **21**, 465 (1965), and associated references.
10. R. L. Bjork, *J. Geophys. Res.* **66**, 3379 (1961).
11. I thank the U.S. Geological Survey for assistance in reviewing the Orbiter photographs, and R. Eggleton, J. W. Hawkins, and M. Bass for helpful discussions. Supported by the U.S. Office of Naval Research under contract Nonr 2216(20).

13 February 1969

Acidic Components of Green River Shale Identified by a Gas Chromatography–Mass Spectrometry–Computer System

Abstract. *A system consisting of a gas chromatograph coupled to a mass spectrometer and computer has been used to characterize the extractable acidic components of Green River shale. This system accumulates mass spectra at every point of the gas chromatogram in a permanent form which permits one to observe mass spectra of minor as well as major constituents. One minor component, whose identification was confirmed by synthesis, was 6,10,14-trimethylpentadecanoic acid.*

Within the past few years, the utilization of gas chromatography for separation and of mass spectrometry for identification has led to significant advances in the characterization of organic mixtures isolated from geological sources. In most of these cases after collection the fraction is introduced into the mass spectrometer; the use of a system in which a gas chromatograph is directly coupled to a mass spectrometer (GC-MS) eliminates the tedious collection of the sample. This technique, which requires a mass spectrometric scan whenever a fraction of interest emerges from the gas chromatograph, still results in an inefficient and rather subjective selection of part of the total material. We have, therefore, explored the possibilities inherent in our recently developed GC-MS computer system (*1*), which permits automatic, continuous (every 4 seconds) recording of the mass spectrum of the effluent of the gas chromatograph. The computer not only serves as a digital recording system, but it can, after appropriate programming, also aid in the interpretation or identification of the large number of spectra thus obtained (about 400 spectra for a gas chromatogram ½ hour in duration).

The major advantage of such a system is that all the information inherent in a GC-MS system is accumulated in permanent form at once, and mass spectra are obtained at every point of the chromatogram rather than only for major or well-resolved components.

Table 1. Minor constituents identified in gas chromatogram of extracted acidic components of Green River shale (Fig. 1).

Label on Fig. 1	Identification
a	Methyl 2,6-dimethylheptanoate
b	2,6,10-Trimethyldodecane*
c	Tetradecane*
d	2,6,10-Trimethyltridecane*
e	Methyl 9-methylpentadecanoate
f	Pentadecane*
g	Hexadecane*
h	Dimethyl octanedioate†
i	2,6,10,14-Tetramethylpentadecane*
j	Heptadecane*
k	2,6,10,14-Tetramethylhexadecane*
l	Nonadecane*; and dimethyl pentanedioate
m	Dimethyl tridecanedioate; and methyl 2,6,10-trimethylhexadecanoate†
n	Methyl 16-methylheptadecanoate
o	Dibutyl phthalate‡
p	Dimethyl tetradecanedioate
r	Dimethyl pentadecanedioate
t	Dimethyl hexadecanedioate
v	Dimethyl heptadecanedioate†
w	Dimethyl octadecanedioate†
x	Dimethyl nonadecanedioate†

* Incompletely removed major component of the neutral fraction of total extract. † Identification tentative. ‡ Artifact also present in procedure blank.